Chemical Engineering Journal 161 (2010) 240–249

Contents lists available at ScienceDirect

Chemical Engineering Journal

journal homepage: www.elsevier.com/locate/cej

Kinetic modeling of propylene homopolymerization in a gas-phase fluidized-bed reactor

Ahmad Shamiri [a], Mohamed Azlan Hussain [a,*], Farouq Sabri Mjalli [a], Navid Mostoufi [b]

[a] Department of Chemical Engineering, University of Malaya, 50603 Kuala Lumpur, Malaysia
[b] Process Design and Simulation Research Center, School of Chemical Engineering, College of Engineering, University of Tehran, P.O. Box 11365/4563, Tehran, Iran

ARTICLE INFO

Article history:
Received 3 October 2009
Received in revised form 21 April 2010
Accepted 21 April 2010

Keywords:
Homopolymerization kinetic model
Fluidized-bed reactor
Propylene polymerization
Ziegler–Natta catalyst

ABSTRACT

A comprehensive mechanistic model describing gas-phase propylene polymerization is developed. The kinetics of polymerization is based on a multiple active site for Ziegler–Natta catalyst. The model considers the polymerization reaction to take place in both bubble and emulsion phases. The developed model was used to predict polymer production rate, number and weight average molecular weights, polydispersity index (PDI) and melt flow index (MFI). Results showed that by increasing the superficial gas velocity from 0.1 to 0.7 m/s the proportion of the polymer produced in the bubble phase increases from 7.92% to 13.14% which highlights the importance of considering the existence of catalyst in the bubble phase. Comparing the developed model with published models of the same reactor revealed that the polymer productivity will be higher using the new model at high catalyst feed rate.

1. Introduction

Bubbling fluidized beds have extensively been studied over the past 50 years and a variety of models have been proposed to describe their steady-state and dynamic behavior [1–6]. The literature shows that the main objective of gas-phase olefin polymerization reaction engineering is to understand how the reaction mechanism, the physical transport processes, reactor configuration and reactor operating conditions affect the properties of the polymer product. In general, polymerization processes can be widely classified into homogeneous and heterogeneous. The homogeneous reactor comprises polymerization which is carried out in just one phase. In the heterogeneous systems, polymerization occurs in the presence of different phases, thus, inter-phase mass transfer, heat transfer and chemical reactions are important.

To describe the kinetic scheme of heterogeneous Ziegler–Natta catalyst, single, as well as multiple, catalyst active sites models have been proposed [7–9]. In this kinetic scheme the key elementary reactions have been established, which include formation of active centers, insertion of monomer into the growing polymer chains, chain transfer reactions, and catalyst deactivation. Most of the proposed mechanisms are based on information about polymerization rate, molecular weight distribution and active center concentrations.

A flow diagram of gas-phase polypropylene production process is shown in Fig. 1. As shown in this figure, Ziegler–Natta catalyst and triethyl aluminum co-catalyst are charged continuously to the reactor and react with the reactants (propylene and hydrogen) to produce the polymer. The feed gas which comprises propylene, hydrogen and nitrogen, provides fluidization through the distributor, heat transfer media and supply reactants for the growing polymer particles. The fluidized particles disengage from unreacted gases in the disengaging zone. The solid-free gas is combined with fresh feed stream after heat removal and recycled back to the gas distributor. The monomer conversion per pass through the bed can vary from 2% to 5% and overall monomer conversion can be as high as 98% [10]. The polypropylene product is continuously withdrawn from near the base of the reactor and above the gas distributor. The unreacted gas is recovered from the product which proceeds to the finishing area of the plant.

Many researchers (e.g., [1,10–13]) have presented various models for gas-phase olefin polymerization in fluidized-bed reactors in order to investigate temperature control problems and to predict system stability. In this work, a dynamic multiple active sites model is presented to describe the kinetic behavior, production rate and molecular weight distribution of propylene homopolymerization, in an industrial-scale gas-phase fluidized-bed reactor. The present model focuses on characterizing the homopolymerization kinetics occurring at the multiple active sites of the catalyst.

2. Polymerization kinetics

Ability of the heterogeneous Ziegler–Natta catalysts to produce polymers with broad molecular weight distributions has

* Corresponding author. Tel.: +60 379675214; fax: +60 379675319.
E-mail address: mohd_azlan@um.edu.my (M.A. Hussain).

1385-8947/$ – see front matter © 2010 Elsevier B.V. All rights reserved.
doi:10.1016/j.cej.2010.04.037

Nomenclature

$AlEt_3$	triethyl aluminum co-catalyst
A_r	Archimedes number
B	moles of reacted monomer bound in the polymer in the reactor
B_w	mass of resin in the reactor (kg)
d_p	particle diameter (m)
Fcat	catalyst feed rate (kg/s)
$F^*_{in}(j)$	molar flow rate of potential active sites of type j into the reactor
H_2	hydrogen
I_m	impurity such as carbon monoxide (kmol/m^3)
j	active site type
$k_{dI}(j)$	deactivation by impurities rate constant for a site of type j
$k_{ds}(j)$	spontaneous deactivation rate constant for a site of type j
$k_f(j)$	formation rate constant for a site of type j
$k_{fh}(j)$	transfer rate constant for a site of type j with terminal monomer M reacting with hydrogen
$k_{fm}(j)$	transfer rate constant for a site of type j with terminal monomer M reacting with monomer M
$k_{fr}(j)$	transfer rate constant for a site of type j with terminal monomer M reacting with $AlEt_3$
$k_{fs}(j)$	spontaneous transfer rate constant for a site of type j with terminal monomer M
$k_h(j)$	rate constant for reinitiation of a site of type j by monomer M
$k_{hr}(j)$	rate constant for reinitiation of a site of type j by co-catalyst
$k_i(j)$	rate constant for initiation of a site of type j by monomer M
$k_p(j)$	propagation rate constant for a site of type j with terminal monomer M reacting with monomer M
M	monomer (propylene)
MFI	melt flow index (g/10 min)
$\overline{M}_n$	number average molecular weight of polymer (kg/kmol)
$\overline{M}_w$	weight average molecular weight of polymer (kg/kmol)
Mw	monomer molecular weight (kg/kmol)
$N^*(j)$	potential active site of type j
$N(0, j)$	uninitiated site of type j produced by formation reaction
$N(1, j)$	living polymer chain of type j with length one
$N(r, j)$	living polymer molecule of length r, growing at an active site of type j, with terminal monomer M
$N_d(j)$	spontaneously deactivated site of type j
$N_{dI}(0, j)$	impurity killed sites of type j
$N_{dIH}(0, j)$	impurity killed sites of type j
$N_H(0, j)$	uninitiated site of type j produced by transfer to hydrogen reaction
NS	number of active site types
P	pressure (Pa)
PDI	polydispersity index
PP	polypropylene
$Q(r, j)$	dead polymer molecule of length r produced at a site of type j
r	number of units in polymer chain
R	instantaneous consumption rate of monomer (kmol/s)
$R(j)$	rate at which monomer M is consumed by propagation reactions at sites of type j
Re_{mf}	Reynolds number of particles at minimum fluidization condition
R_p	production rate (kg/s)
R_{pb}	bubble phase production rate (kg/s)
R_{pe}	emulsion phase production rate (kg/s)
R_v	volumetric polymer outflow rate from the reactor (m^3/s)
t	time (s)
T	temperature (K)
U_0	superficial gas velocity (m/s)
U_{mf}	minimum fluidization velocity (m/s)
V	reactor volume (m^3)
V_b	volume of bubbles
V_p	volume of polymer phase in the reactor (m^3)
V_{pb}	volume of polymer phase in the bubble phase (m^3)
V_{pe}	volume of polymer phase in the emulsion phase (m^3)
$X(n, j)$	nth moment of chain length distribution for dead polymer produced at a site of type j
$Y(n, j)$	nth moment of chain length distribution for living polymer produced at a site of type j

Greek letters

δ	volume fraction of bubbles in the bed
ε_b	void fraction of bubble for Geldart B particles
ε_e	void fraction of emulsion for Geldart B particles
ε_{mf}	void fraction of the bed at minimum fluidization
μ	gas viscosity (Pa s)
ρ_g	gas density (kg/m^3)
ρ_s	polymer density (kg/m^3)

long being recognized. There are two factors responsible for exhibiting this distribution. One factor is mass and heat transfer resistances that lead to a broadening of the molecular weight distribution. The other factor is existence of multiple sites where each type has its own relative reactivity. However, it has been shown that under most polymerization conditions, the effect of multiple active site types is more important than that of transport resistances [14,15]. The single-site kinetic model is not enough to describe the kinetic behavior, production rate and molecular weight distribution of propylene homopolymerization. Therefore, a two-type active site was considered in the present study.

Using a similar methodology to McAuley et al. [9], Kissin [16] and Carvalho de et al. [17], the following kinetic model was developed using Ziegler–Natta catalysts containing multiple active sites to describe the homopolymer production rate, molecular weight and its distribution. Throughout this section, the index j refers to the type of active site. Each site type is associated with different rate constants for formation, initiation, propagation and chain transfer. The following reactions were considered for the Ziegler–Natta multi-site catalyst.

2.1. Formation of active sites

For a typical Ziegler–Natta catalyst potential active sites of type j on the catalyst particle and the co-catalyst react to form active sites [16]:

$$N^*(j) + \text{co-catalyst} \xrightarrow{k_f(j)} N(0, j) \quad (1)$$

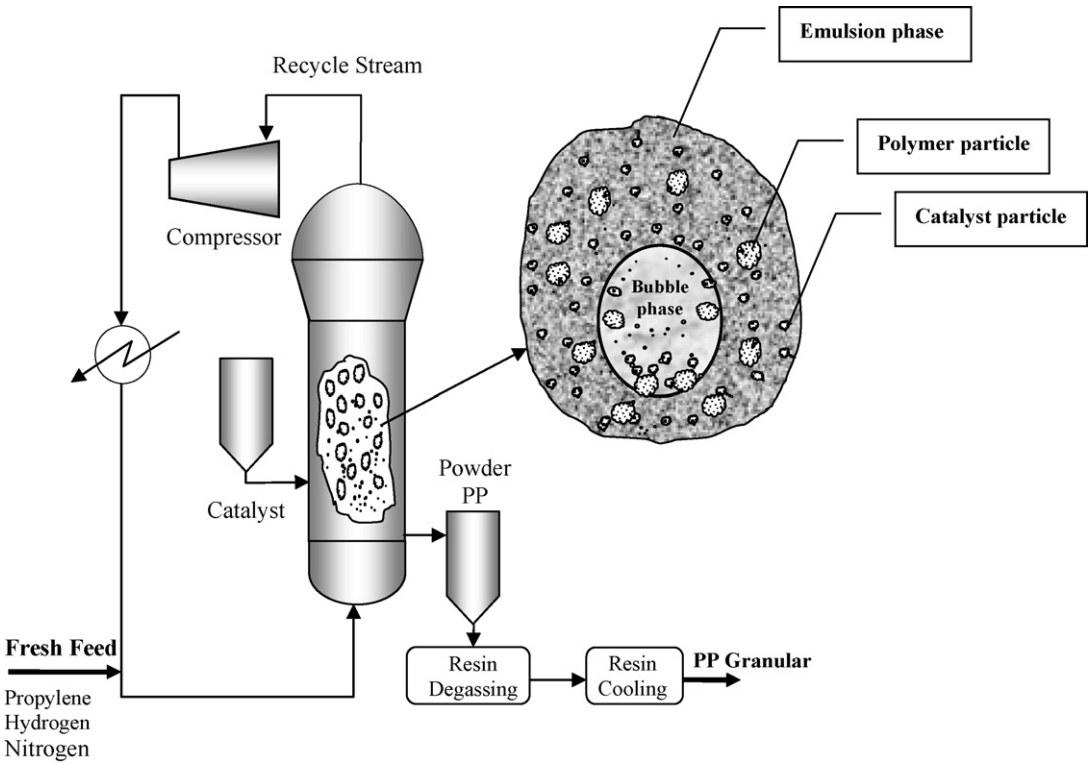

Fig. 1. Schematic of an industrial fluidized-bed polypropylene reactor.

2.2. Initiation of active sites

The active sites react with the monomer to form propagation sites:

$$N(0,j) + M \xrightarrow{k_i(j)} N(1,j) \quad (2)$$

2.3. Propagation

The propagation sites support the growth of living polymer chains. Addition of fresh monomer molecules to active sites increase the length of the chain by one unit as indicated below:

$$N(r,j) + M \xrightarrow{k_p(j)} N(r+1,j) \quad (3)$$

2.4. Chain transfer reactions

Chain transfer reactions occur with monomers, hydrogen, co-catalyst and spontaneous transfer reactions [16]. These chain transfer reactions are described in more details below.

2.4.1. Transfer to monomer

Chain transfer to monomer reactions can be expressed as:

$$N(r,j) + M \xrightarrow{k_{fm}(j)} N(1,j) + Q(r,j) \quad (4)$$

where $Q(r, j)$ is a dead polymer segment of length r which cannot undergo any further reactions. The living polymer chains of length one, $N(1, j)$, can propagate to form new polymer chains.

2.4.2. Transfer to hydrogen

The main transfer step in industrial propylene polymerization is the transfer to hydrogen. Varying hydrogen concentration in the reactor is the main technique to control molecular weight averages of industrial polypropylene resin.

$$N(r,j) + H_2 \xrightarrow{k_{fh}(j)} N_H(0,j) + Q(r,j) \quad (5)$$

$$N_H(0,j) + M \xrightarrow{k_h(j)} N(1,j) \quad (6)$$

These sites become quickly reinitiated by reacting with the co-catalyst. If the co-catalyst is triethyl aluminum, the reinitiation reaction is given by [16]:

$$N_H(0,j) + AlEt_3 \xrightarrow{k_{hr}(j)} N(1,j) \quad (7)$$

2.4.3. Transfer to co-catalyst

For particular reactor operation conditions, especially at elevated polymerization temperatures, transfer to co-catalyst may be considerable. It is, however, generally negligible at normal polymerization temperatures with Ziegler–Natta catalysts [18].

$$N(r,j) + AlEt_3 \xrightarrow{k_{fr}(j)} N(1,j) + Q(r,j) \quad (8)$$

2.4.4. Spontaneous transfer

Spontaneous transfer reactions can be described as:

$$N(r,j) \xrightarrow{k_{fs}(j)} N_H(0,j) + Q(r,j) \quad (9)$$

This site can undergo initiation reactions with monomer as for transfer to hydrogen.

2.5. Deactivation reactions

Active sites may deactivate spontaneously to generate dead sites and dead polymer chains that are unable to catalyze polymerization:

$$N(r,j) \xrightarrow{k_{ds}(j)} N_d(j) + Q(r,j) \quad (10)$$

$$N(0,j) \xrightarrow{k_{ds}(j)} N_d(j) \quad (11)$$

$$N_H(0,j) \xrightarrow{k_{ds}(j)} N_d(j) \quad (12)$$

Table 1
Differences between the present model and the previously models.

No.	Function	Present model	Harshe et al. [6]	Zacca et al. [5]
1	Phases	Bubble and emulsion phases	Bubble and emulsion phase	Only one phase (well mixed)
2	Chemical reaction	Chemical reaction occurs in emulsion and bubble phase	Chemical reaction occurs only in the emulsion phase	Chemical reaction occurs in one phase
3	Rate of reaction	Activation, initiation, propagation, chain transfer to monomer, chain transfer to hydrogen, chain transfer to co-catalyst, spontaneous chain transfer, spontaneous deactivation and reaction with poisons	Propagation, spontaneous deactivation and site transformation reactions	Propagation, spontaneous deactivation and site transformation reactions

2.6. Reactions with poisons

Existence of catalyst poisons in the polymerization system is considered as one of the worst conditions in industrial polymerization processes. One of the functions of alkyl aluminum catalysts is to passivate the system by removing most of the polar poisons in the reactor prior to catalyst injection and polymerization. Even low levels of some reactive impurities, such as carbon monoxide, can cause a nearly instantaneous drop in propagation rates. Adsorption of such an impurity onto a catalyst site can cause it inactive. These reactions can be shown as follows:

$$N(r,j) + I_m \xrightarrow{k_{dI}(j)} N_{dIH}(0,j) + Q(r,j) \quad (13)$$

$$N_H(0,j) + I_m \xrightarrow{k_{dI}(j)} N_{dIH}(0,j) \quad (14)$$

$$N(0,j) + I_m \xrightarrow{k_{dI}(j)} N_{dI}(0,j) \quad (15)$$

3. Model development

A mathematical model based on the previously explained kinetic system was derived in the present study. This model consists of mass balances on the species present in the reactor and a series of algebraic and differential equations presented in the next subsection. Characterization of polymer properties is modeled using the population balances and method of moments. Application of population balances and the method of moments allows for the prediction of the physiochemical characteristics of the polymer such as molecular weight, polydispersity index (PDI), melt flow index (MFI), density, polymer production rate, monomer conversion and active site information. In the method of moments, moments of the chain length distribution are calculated for living and dead polymer. These moments are then used to calculate molecular weight or chain length averages of the polymer produced in the reactor.

The assumptions considered in developing the model are summarized below:

- The fluidized bed comprises of two phases: bubble and emulsion.
- The emulsion phase is not at the minimum fluidization condition and the bubbles contain solid particles.
- Reactions occur in both bubble and emulsion phases.
- There is negligible resistance to heat and mass transfer between the gas and polymer particles due to small catalyst particles, low to moderate catalyst activity or polymerization rates [19].
- Constant mean particle size is assumed throughout the bed.
- A two-site kinetic scheme is assumed.

The difference between developed model and previously reported models is shown in Table 1.

3.1. Mass balance equations for active sites and reacted monomers

The mass balance on the number of moles of potential active sites $N^*(j)$ in the reactor is given by:

$$\frac{dN^*(j)}{dt} = F^*_{in}(j) - k_f(j)N^*(j) - N^*(j)\frac{R_v}{V_p} \quad (16)$$

The molar flow rate of potential active sites into the reactor $F^*_{in}(j)$ is proportional to the mass feed rate of the catalyst. The volumetric flow rate of polymer from the reactor is R_v and the volume of the polymer phase in the reactor is V_p. Similarly, the following equations can be written for the number of moles of initiation sites N(0, j) and $N_H(0,j)$:

$$\frac{dN(0,j)}{dt} = k_f(j)N^*(j) - N(0,j)\left\{k_i(j)[M] + k_{ds}(j) + k_{dI}(j)[I_m] + \frac{R_v}{V_p}\right\} \quad (17)$$

$$\frac{dN_H(0,j)}{dt} = Y(0,j)\{k_{fh}(j)[H_2] + k_{fs}(j)\} - N_H(0,j) \times \left\{k_h(j)[M] + k_{ds}(j) + k_{h_r}(j)[AlEt_3] + k_{dI}(j)[I_m] + \frac{R_v}{V_p}\right\} \quad (18)$$

In these equations [M] *is* the molar monomer (propylene) concentration and [H_2] is the concentration of hydrogen. $Y(0, j)$ *is* the zeroth moment of the living polymer chain length distribution given as:

$$Y(0,J) = \sum_{r=1}^{\infty}\{N(r,j)\} = N(1,j) + \sum_{r=2}^{\infty}N(r,j) \quad (19)$$

The population balance for living chains growing on active sites of length $r = 1$ is given by:

$$\frac{dN(1,j)}{dt} = k_i(j)N(0,j)[M] + N_H(0,j)\{k_h(j)[M] + k_{hr}(j)[AlEt_3]\} + Y(0,j)\{k_{fm}(j)[M] + k_{fr}(j)[AlEt_3]\} - N(1,j) \times \left\{k_p(j)[M] + k_{fm}(j)[M] + k_{fh}(j)[H_2] + k_{fr}(j)[AlEt_3] + k_{fs}(j) + k_{ds}(j) + k_{dI}(j)[I_m] + \frac{R_v}{V_p}\right\} \quad (20)$$

For the living chains with length greater than 1, $r \geq 2$, the equivalent population balance is:

$$\frac{dN(r,j)}{dt} = k_p(j)[M]N(r-1,j) - N(r,j) \left\{k_p(j)[M] + k_{fm}(j)[M] + k_{fr}(j)[AlEt_3] + k_{fh}(j)[H_2] + k_{fs}(j) + k_{ds}(j) + k_{dI}(j)[I_m] + \frac{R_v}{V_p}\right\} \quad (21)$$

Population balances for dead chains (for $r \geq 2$) are as follows:

$$\frac{dQ(r,j)}{dt} = N(r,j)\{[M]k_{fm}(j) + [H_2]k_{fh}(j) + [AlEt_3]k_{fr}(j) + k_{fs}(j) + k_{ds}(j) + k_{dI}(j)[I_m]\} - \frac{R_v}{V_p}Q(r,j) \quad (22)$$

The zeroth moment (number of chains) of the chain length distribution for the living polymer chain is given by equation (19). Therefore:

$$\frac{dY(0,j)}{dt} = \frac{d(\sum_{r=1}^{\infty}\{N(r,j)\})}{dt} = \frac{dN(1,j)}{dt} + \sum_{r=2}^{\infty}\frac{dN(r,j)}{dt} \quad (23)$$

where

$$\sum_{r=2}^{\infty}N(r-1,j) = \sum_{r=1}^{\infty}N(r,j) = Y(0,j) \quad (24)$$

By substituting Eqs. (20) and (21) into Eq. (23) and summation over all r values, the following mass balance on $Y(0, j)$, the zeroth moment of the living polymer chain length distribution can be obtained:

$$\frac{dY(0,j)}{dt} = [M]\{k_i(j)N(0,j) + k_h(j)N_H(0,j)\} + N_H(0,j)k_{hr}(j)[AlEt_3] - Y(0,j)\left\{k_{fh}(j)[H_2] + k_{fs}(j) + k_{ds}(j) + k_{dI}(j)[I_m] + \frac{R_v}{V_p}\right\} \quad (25)$$

Mass balances on the first and second moments of the living polymer distribution can be determined as well:

$$\frac{dY(1,j)}{dt} = \frac{d(\sum_{r=1}^{\infty}r\{N(r,j)\})}{dt} = \frac{dN(1,j)}{dt} + \sum_{r=2}^{\infty}r\frac{dN(r,j)}{dt}$$
$$= [M]k_i(j)N(0,J) + N_H(0,J)\{k_h(j)[M] + k_{hr}(j)[AlEt_3]\} + Y(0,j)\{k_{fm}(j)[M] + k_{fr}(j)[AlEt_3]\} + [M]k_p(j)Y(0,j) - Y(1,j)\left\{k_{fm}(j)[M] + k_{fr}(j)[AlEt_3] + k_{fh}(j)[H_2] + k_{fs}(j) + k_{ds}(j) + k_{dI}(j)[I_m] + \frac{R_v}{V_p}\right\} \quad (26)$$

where

$$\sum_{r=2}^{\infty}r\{N(r-1,j)\} = \sum_{r=1}^{\infty}(r+1)N(r,j) = Y(1,j) + Y(0,j) \quad (27)$$

Noting that:

$$\sum_{r=2}^{\infty}r^2\{N(r-1,j)\} = \sum_{r=1}^{\infty}(r+1)^2N(r,j) = Y(2,j) + 2Y(1,j) + Y(0,j) \quad (28)$$

$$\frac{dY(2,j)}{dt} = \frac{d(\sum_{r=1}^{\infty}r^2\{N(r,j)\})}{dt} = \frac{dN(1,j)}{dt} + \sum_{r=2}^{\infty}r^2\frac{dN(r,j)}{dt}$$
$$= [M]k_i(j)N(0,j) + N_H(0,j)\{k_h(j)[M] + k_{hr}(j)[AlEt_3]\} + Y(0,j)\{k_{fm}(j)[M] + k_{fr}(j)[AlEt_3]\} + [M]k_p(j)\{2Y(1,j) + Y(0,j)\} - Y(2,j)\left\{k_{fm}(j)[M] + k_{fr}(j)[AlEt_3] + k_{fh}(j)[H_2] + k_{fs}(j) + k_{ds}(j) + k_{dI}(j)[I_m] + \frac{R_v}{V_p}\right\} \quad (29)$$

In the above equations $Y(n, j)$ is the nth moment of the living polymer chain length distribution, which is given by:

$$Y(n,j) = \sum_{r=1}^{\infty}r^n[N(r,j)] \quad n = 1, 2, \ldots \quad (30)$$

The moments of the dead polymer distribution are defined by:

$$X(n,j) = \sum_{r=1}^{\infty}r^nQ(r,j) \quad (31)$$

Similar equations can be derived for the nth moments of the chain length distributions for dead polymer chains by substituting Eqs. (22) and (30) into Eq. (31) and summation over all r values:

$$\frac{dX(n,j)}{dt} = Y(n,j)\{k_{fm}(j)[M] + k_{fr}(j)[AlEt_3] + k_{fh}(j)[H_2] + k_{fs}(j) + k_{ds}(j) + k_{dI}(j)[I_m]\} - X(n,j)\frac{R_v}{V_p} \quad (32)$$

The mass balances for the moments of the dead polymer chain length, distribution were obtained by writing a mass balance on dead polymer segments of length r and substituting the result into the definition for the moments given above.

For predicting the homopolymer composition in the reactor at any time, mass balances for reacted monomers were developed on the number of moles of each type of monomer bound in the polymer particles:

$$\frac{dB}{dt} = R - B\frac{R_v}{V_p} \quad (33)$$

Table 2
Rate constants of the reactions.

Reaction	Rate constant	Unit	Site Type 1	Site Type 2	Reference
Formation	$k_f(j)$	s^{-1}	1	1	[9]
Initiation	$k_i(j)$	l/mol s	22.88	54.93	[20]
	$k_h(j)$	l/mol s	0.1	0.1	[9]
	k_{h_r}	l/mol s	20	20	[9]
Propagation	$k_p(j)$	l/mol s	342.8	34.28	[5]
Transfer	$k_{fm}(j)$	l/mol s	0.0865	0.2171	[20]
	$k_{fh}(j)$	l/mol s	7.5	7.5	[20]
	$k_{fr}(j)$	l/mol s	0.024	0.12	[9]
	$k_{fs}(j)$	l/mol s	0.0001	0.0001	[9]
Deactivation	$k_{ds}(j)$	s^{-1}	0.00034	0.00034	[20]
	$k_{dI}(j)$	l/mol s	2000	2000	[9]

In this equation B is the number of moles of monomer which are incorporated in the polymer in the reactor and R is the instantaneous consumption rate of monomer to form polymer. Assuming that the only significant consumption of monomers is by propagation, the following expression for consumption rate can be obtained:

$$R = \sum_{j=1}^{NS} [\mathrm{M}] Y(0,j) k_p(j) \tag{34}$$

The volumetric outflow rate of polymer, R_v, can be determined from the consumption rates of the monomers and the rate of change of the weight of polymer in the reactor:

$$R_v = \frac{MwR}{\rho_s} - \frac{dB_w/dt}{\rho_s} \tag{35}$$

3.2. Homopolymer properties

The number average and weight average molecular weights, $\overline{M}_n$ and $\overline{M}_w$, can be determined using the method of moments as follows:

$$\overline{M}_n = Mw \left(\frac{\sum_{j=1}^{NS} (X(1,j) + Y(1,j))}{\sum_{j=1}^{NS} (X(0,j) + Y(0,j))} \right) \tag{36}$$

$$\overline{M}_w = Mw \left(\frac{\sum_{j=1}^{NS} (X(2,j) + Y(2,j))}{\sum_{j=1}^{NS} (X(1,j) + Y(1,j))} \right) \tag{37}$$

The PDI is defined by the ratio of weight average to number average molecular weights:

$$\mathrm{PDI} = \frac{\overline{M}_w}{\overline{M}_n} \tag{38}$$

The instantaneous mass rate production of polymer at sites of type j is expressed as:

$$R_p(j) = Mw[\mathrm{M}] Y(0,j) k_p(j) \tag{39}$$

Control of MFI is an important issue for producing desired polypropylene grade. MFI of polymer is a function of its molecular weight, which is related to the operating conditions of the reactor and the feed composition. The relation between MFI and the weight average molecular weights of polypropylene is given by [9]:

$$\mathrm{MFI} = 3.346 \times 10^{17} \overline{M}_w^{-3.472} \tag{40}$$

3.3. Reaction rate constants

The reaction rate constants used in this work were taken from different published works on similar reactive systems [5,9,20]. This is mainly due to the lack of a unique source that covers all the kinetic parameters for propylene polymerization. Predictions were generated using the rate constants given in Table 2. The constants from Table 2 provide reasonable predictions. It is worth mentioning that formation, initiation, chain transfer and deactivation reaction rate constants were taken from polyethylene literature. The rate of these reactions are mainly related to the catalyst and not affected directly by the type of monomer. Moreover, it was shown that changes in the rate constants of formation, initiation, transfer to co-catalyst, spontaneous transfer and spontaneous catalyst deactivation reaction has marginal influence on the model predictions [9]. Hence, assuming similar values for these rate constants as the case of polyethylene is reasonable. In the present study, effect of temperature (thus activation energies) on the polymerization kinetics was not considered, as all the simulations in this work were done at constant bed temperature. It has been established that under various conditions, when the catalyst particles are sufficiently small and the catalyst activity is not extremely high (low to moderate polymerization rates), mass and heat transfer resistances inside the polymer particle and between the gas and the solid polymer particles do not play an important role and will not significantly affect the dynamic behavior of the reactor and the overall properties of the polyolefin [5,8,10,19]. Therefore, the temperature inside the particles (where the reactions take pace) is practically the same as the bed temperature.

From the simulations, it was determined that the model prediction of production rate is most sensitive to changes in the rate constants for propagation, transfer to hydrogen, spontaneous transfer and deactivation reaction. Polymer properties are influenced by propagation, transfer to hydrogen, spontaneous transfer, transfer to monomer and deactivation reaction rate constants. Formation, initiation and transfer to co-catalyst reaction rate constants had very little influence on the model predictions. Deactivation rate constants for impurities are important when carbon monoxide is presented in the reactor.

Table 3
Empirical correlations used in the developed model.

Formula	Reference
$Re_{mf} = \left[(29.5)^2 + 0.357Ar\right]^{1/2} - 29.5$	[29]
$Ar = \frac{\rho_g(\rho_s - \rho_g) g d_p^3}{\mu_g^2}$	
$\delta = 0.534 \left[1 - \exp\left(-\frac{U_0 - U_{mf}}{0.413}\right)\right]$	[22]
$\varepsilon_e = \varepsilon_{mf} + 0.2 - 0.059 \exp\left(-\frac{U_0 - U_{mf}}{0.429}\right)$	[22]
$\varepsilon_b = 1 - 0.146 \exp\left(-\frac{U_0 - U_{mf}}{4.439}\right)$	[22]
$V_{Pe} = Ah(1 - \varepsilon_e)(1 - \delta)$	
$V_{Pb} = Ah(1 - \varepsilon_b)\delta$	

3.4. Reactor hydrodynamics

The simple two-phase flow structure for the gas-phase olefin polymerization model has been used previously in the literature [1,6,10,21]. This model assumes the existence of solid-free bubbles in the fluidized bed while the emulsion remains at minimum fluidization conditions. However, the voidage of the emulsion phase may differ far from that at the minimum fluidization. Moreover, the bubbles may contain different portions of solids [22]. Based on this concept, Cui et al. [22] proposed the dynamic two-phase structure (particle concentration in emulsion and bubbles varies with gas velocity) for the fluidized-bed hydrodynamics. Since the assumption of the minimum fluidization condition for the emulsion phase in the polypropylene reactor (simple two-phase model) is not realistic [23], the dynamic two-phase flow structure of fluidized beds, proposed by Cui et al. [22], was used in this study to calculate a better estimation of the average bed voidage. The constants of Cui et al. [22] correlations (Table 3) were selected for polypropylene Geldart B particles, produced in the reactor. The correlations required for estimating the void fractions of bubble and emulsion phases from the dynamic two-phase model are summarized in Table 3.

Cui et al. [22] provided the constants of dynamic two-phase model for FCC and sand as representative of Geldart A and Geldart B particles. Polypropylene particles are Geldart B, thus, the constants of this type of particles were chosen and shown in Table 3. It is worth noting that the same approach was adopted in similar modeling attempts and shown that this model provides good results [3,4,23–26].

Table 4
Operating conditions and physical parameters considered in this work for modeling fluidized-bed polypropylene reactors.

Operating conditions	Physical parameters
V (m^3) = 50	μ (Pa s) = 1.14×10^{-4}
T_{ref} (K) = 353.15	ρ_g (kg/m^3) = 23.45
T_{in} (K) = 330.15	ρ_s (kg/m^3) = 910
P (bar) = 25	dp (m) = 500×10^{-6}
Propylene concentration (mol/l) = 1.267	
Hydrogen concentration (mol/l) = 0.02	
Catalyst feed rate (g/s) = 0.2	

3.5. Model solution

In order to reduce the computational efforts for solution of the model, the steady-state assumption was made for $N^*(j)$, $N(0, j)$, $N_H(0, j)$ and $N(1, j)$ species. The set of Eqs. (16), (17), (18) and (20) is stiff because the dynamics associated with changes in the intermediate species are very fast compared to the dynamics associated with the other states in the model [9]. Therefore, the corresponding differential equations were converted to algebraic equations by setting the left-hand-side derivative terms to zero. The set of model equations were solved numerically using MATLAB.

4. Results and discussion

The model developed in this work was used to evaluate the performance of the fluidized-bed reactor of propylene homopolymerization. A two-site kinetic scheme was used in the development of the model. In order to demonstrate the predictive capabilities of the proposed model, simulations were carried out at the operating conditions shown in Table 4. Using the dynamic two-phase hydrodynamic model, it is possible to show that the emulsion phase contains about 88% of the catalyst while the bubbles carry about 12% of the catalyst introduced into the reactor [3,27,28]. Therefore, the reaction rate is higher in the emulsion than in the bubble phase.

However, the portion of reaction occurring in the bubbles is of appreciable amount and need to be considered in the model.

It is worth noting that no experimental data were found for the conditions of this work. Of course, some polymer properties can be found for industrial polypropylene grades but the operating conditions of the reactors in which these products have been produced have not been revealed. Thus, due to lack of experimental data, the model was tested against the simulation results of Zacca et al. [5] and Harshe et al. [6]. In the model proposed by Zacca et al. [5] only time-dependent reaction mechanisms were considered that were first order with respect to catalyst sites and in the model proposed by Harshe et al. [6], the kinetic scheme of Hutchinson et al. [8] was used.

Fig. 2 compares the model developed in this work with the models of Zacca et al. [5] and Harshe et al. [6] in terms of the effect of catalyst feed rate on the production capacity. It can be seen from this figure that the predicted results obtained by the new model agree reasonably well with the results reported by Zacca et al. [5] and Harshe et al. [6]. Fig. 2 shows that at high increasing catalyst feed rate, the polymer production rate predicted by the new model becomes greater than that obtained by the previous models. This is mainly due to the consideration of reactions in the bubble phase which will result in more polymer production. In fact, the previous models have neglected the amount of catalyst in the bubbles. In other words, more reaction volume is available in reality compared to the previous two models, namely, volume of polymer in the bubble phase (V_{pb}) and volume of polymer in the emulsion phase (V_{pe}). Hence, the reaction capacity of the previous models is lower than

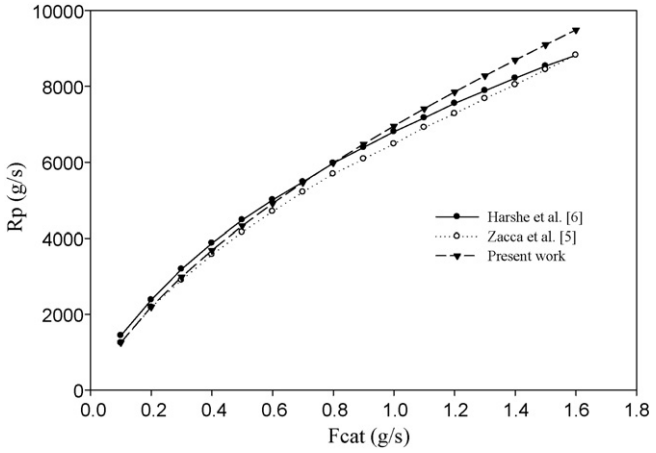

Fig. 2. The present model polymer production rate as compared to previously reported models.

the present one. This becomes clearer at higher catalyst feed flow rate. The model was then used to investigate the effect of various operating parameters such as superficial gas velocity, catalyst feed rate and hydrogen concentration on the performance of the fluidized-bed polypropylene reactor.

4.1. Polymer production rate

Calculated overall production rate of polymer in the reactor as well as the production rates of polymer in the bubble and emulsion phases over the time is shown in Fig. 3. Obviously, the overall production rate of polypropylene in the bubble phase is less than that in the emulsion phase due to lower amount of catalyst presented in the bubble phase compared to the emulsion phase. Share of the production rates of the polymer in the emulsion and bubble phases are roughly 88% and 12%, respectively. This clearly indicates that contribution of the catalyst inside the bubble phase should not be neglected in any modeling attempt [3]. It is worth noting that this considerable amount of polymerization in the bubbles was ignored in all previous gas-phase propylene polymerization models reported in the literature.

Fig. 4 illustrates the effect of impurity (carbon monoxide) on production rate. As can be seen, the propylene polymerization rate sharply decreases by carbon monoxide injection. Increasing the concentration of carbon monoxide results in further decrease in the polymerization rate.

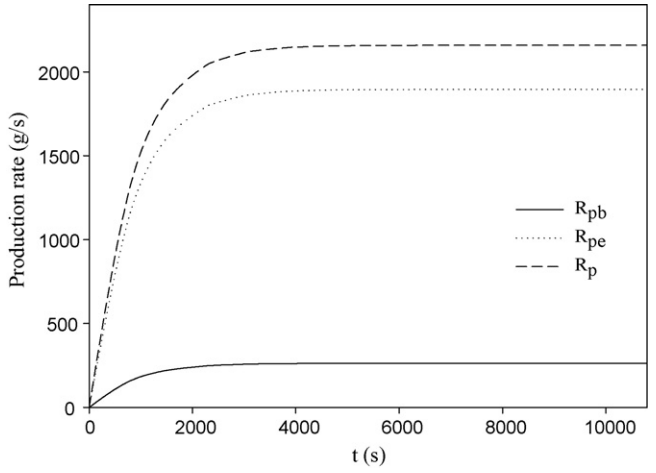

Fig. 3. Evolution of production rate of the polymer over the time in the reactor (Fcat = 0.2 g/s and U_0 = 0.35 m/s).

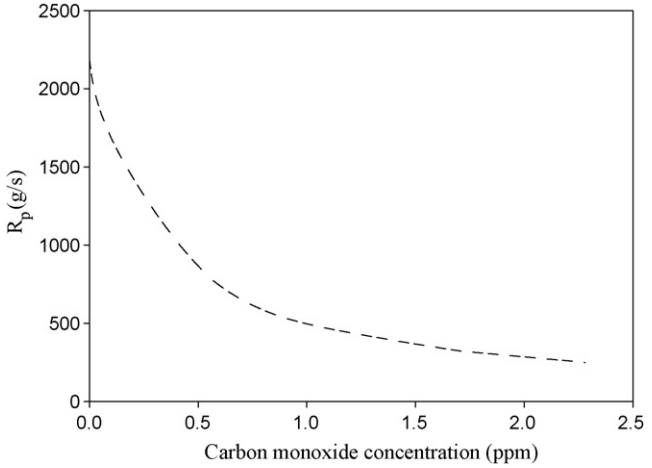

Fig. 4. Effect of impurity (CO) on production rate (Fcat = 0.2 g/s and U_0 = 0.35 m/s).

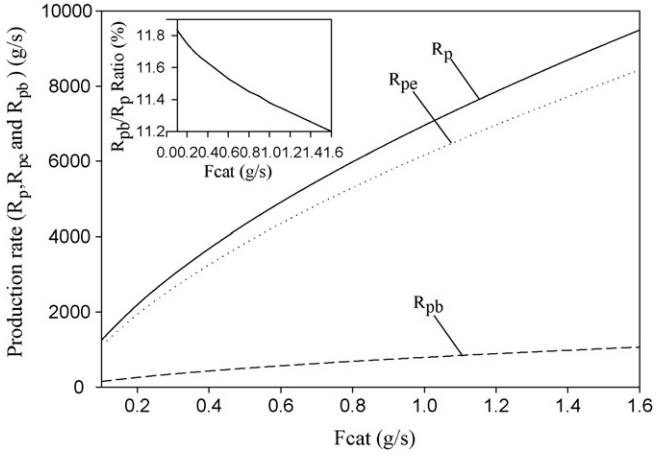

Fig. 6. Effect of Fcat on polymer production rate (in emulsion and bubble phases) at U_0 = 0.35 m/s.

Influence of superficial gas velocity on polypropylene product rate and its distribution in the emulsion and bubble phases is illustrated in Fig. 5. It is worth mentioning that the feed composition (mole fraction of the components) was kept constant in this case. This figure shows that increasing the superficial gas velocity results in decreasing the polymer production rates in emulsion phase, bubble phase and total. Based on the dynamic two-phase correlations given in Table 3, an increase in the superficial gas velocity increases the emulsion and the bubble phase void fractions and velocities which lead to reducing the volume of polymer in the bubble phase (V_{pb}) and the emulsion phase (V_{pe}). Therefore, the monomer mean residence time (total volume of monomer in the reactor divided by the flow rate of monomer at the inlet condition of the reactor) is reduced, resulting in decreasing the total monomer conversion and polymer production rate. An increase in the superficial gas velocity from 0.1 to 0.7 m/s increases the ratio of production of polymer in the bubble phase to the total production rate (R_{pb}/R_p) from 7.92% to 13.14%. Considering the practical superficial gas velocity range of 0.3–0.6 m/s, the bubble contribution to the reaction rate is 11.8–13% which is a considerable amount that should be considered in the model. By increasing the superficial gas velocity, more gas and solid particles enter the bubbles, resulting in increasing the bubble contribution to the reaction rate. However, at high superficial gas velocity, the residence time of solids in the bubble phase (total volume of solids in the bubbles divided by the flow rate of solids entering bubbles at the reactor inlet) is reduced which affects the activity of the solid catalyst inside the bubble phase and, consequently, gives a reduction in polymer production.

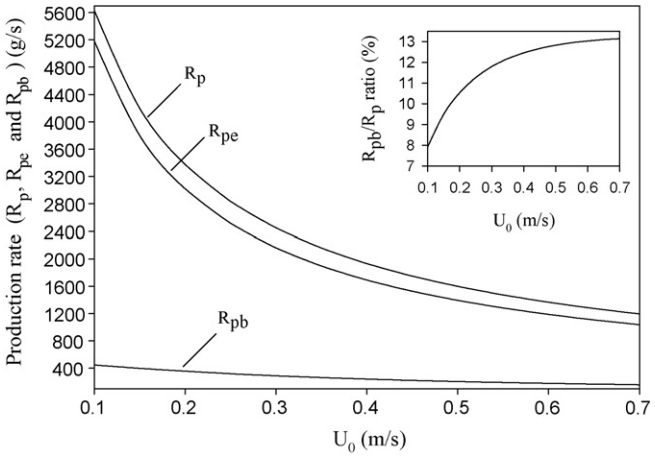

Fig. 5. Effect of superficial gas velocity on polymer production rate (in emulsion and bubble phases) at Fcat = 0.2 g/s.

Fig. 6 shows the effect of catalyst feed rate on polypropylene production rate and its distribution in the emulsion and bubble phases. It can be seen in this figure that by increasing the catalyst feed rate, the polymer production rate increases. An increase in the catalyst feed rate from 0.1 to 1.6 g/s reduces the ratio of the bubble phase production rate to the total production rate of polymer (R_{pb}/R_p) from 11.8% to 11.2%. The results shown in Figs. 5 and 6 reveal that varying the effect of catalyst feed rate is insignificant on the total production ratio. On the other hand, the superficial gas velocity has a profound effect on the gas flow hydrodynamics which results in a greater variation in the total production rate ratio.

4.2. Polymer properties

Molecular weight of polymer and its distribution affects most of the essential properties of polypropylene based on which a good end product can be determined. Small variations in the molecular structure may improve or impair the polymer properties such as tensile strength, thermal stability, stiffness, hardness, softening point and impact strength considerably. The molecular weight distribution provides a general picture of the ratio of large, medium and small molecular chains in the polymer. The PDI is used as a measure of the breadth of the molecular weight distribution. Molecular weight of the polymer also governs the melt flow index.

The most commonly used test or indicator for flow characteristic is the MFI which offers an assessment of average molecular weight and is an inverse measure of the melt viscosity. In other words, the higher MFI, the more polymer flows under test conditions. Knowing MFI of a polymer is vital to anticipate and control of its processing. Generally, polymers with higher MFI are used in injection molding, while polymers with lower MFI are used in blow molding or extrusion processes.

Fig. 7 shows the molecular weight distribution of the polypropylene product as a function of time. This figure illustrates that the number and weight average molecular weight of the polymer increase rapidly at the beginning of the polymerization and reaches a constant value within less than an hour of start of the production.

PDI has the same profile as that of average molecular weight during the course of polymerization. Evolutions of this parameter and MFI with the time are illustrated in Fig. 8. The final value of the PDI, under the conditions of this simulation, is stabilized close to 4.4. This indicates that the produced polypropylene attains a narrow molecular weight distribution. In general, a narrow distribution results in a more regular and repeatable production characteristics.

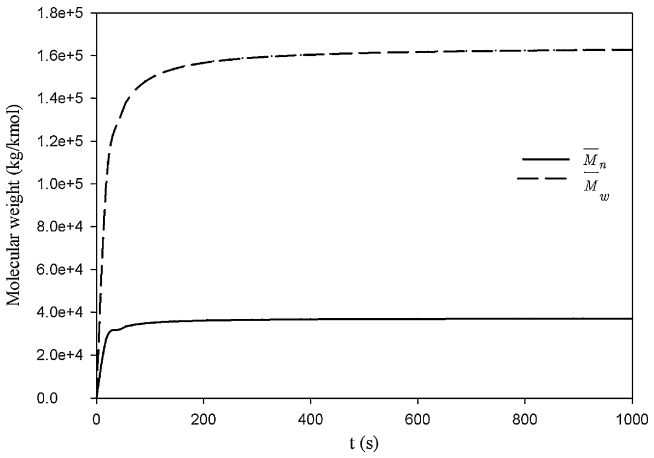

Fig. 7. Evolution of number and weight average molecular weights as a function of time in the reactor (Fcat = 0.2 g/s and U_0 = 0.35 m/s).

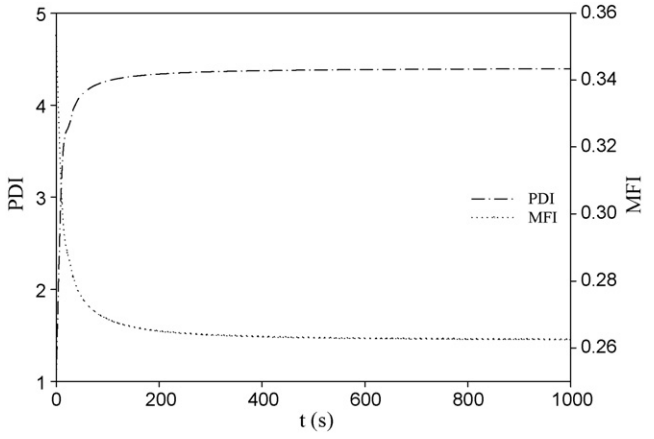

Fig. 8. Evolution of polydispersity index and melt flow index with the time in the reactor (Fcat = 0.2 g/s and U_0 = 0.35 m/s).

Varying hydrogen concentration in the reactor is the most effective technique to control molecular weight averages of industrial polypropylene. Effect of hydrogen concentration on MFI and the PDI of the polymer is shown in Fig. 9. It can be seen that by increasing the hydrogen concentration, the polymer MFI increases, while the PDI decreases exponentially. By injecting more hydrogen, the molecular weights decrease which results in decreasing the chain length and the degree of polymerization due to the increase of chain transfer reaction rate. Reduction in the weight average and number average molecular weights leads to an increase in the polymer MFI and a decrease in the PDI. This is in accordance with the industrial findings for polypropylene production [18].

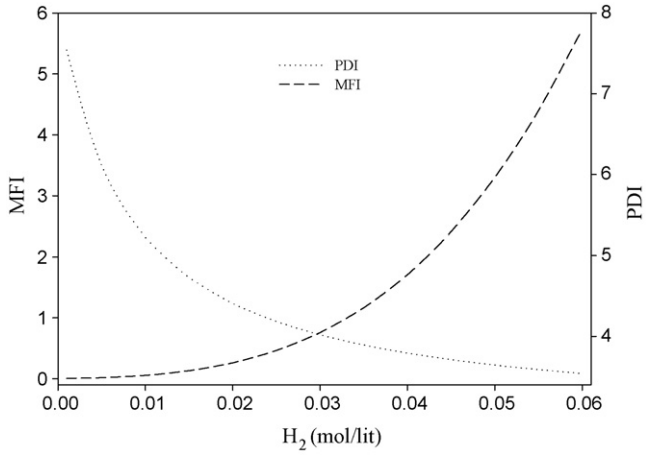

Fig. 9. Effect of hydrogen concentration on MFI and PDI (Fcat = 0.2 g/s and U_0 = 0.35 m/s).

5. Conclusions

A dynamic kinetic model for the production of polypropylene in a gas-phase fluidized-bed reactor was developed in this work. The hydrodynamics of the fluidized-bed reactor of polypropylene production was based on the dynamic two-phase concept of fluidization. This hydrodynamic model was combined with a structured kinetic model to provide a better understanding of the reactor performance. In this model two types of active sites on the heterogeneous Ziegler–Natta catalyst were considered. It was shown that a two-site model can predict the changes in production rate, number and weight average molecular weights, PDI and MFI in an industrial reactor. This model is capable of predicting essential reactor parameters such as polymer productivity of the reactor as well as properties of the produced polymer such as average molecular weight, PDI and molecular weight distribution of polymer. The proposed model was used to study the effects of operating, kinetic and hydrodynamic parameters on the reactor performance as well as polymer properties. Since the bubbles were considered to contain solids, polymerization reactions were occurred not only in the emulsion phase but also inside the bubbles. Results of the proposed model were compared with the results reported by Zacca et al. [5] and Harshe et al. [6] for the polymer production rate. The simulated production rate profile showed a trend very similar to the previously reported models. However, at high catalyst flow rate, the proposed model departs slightly from the previous models, due to the consideration of reactions in the bubble phase.

It was shown that by increasing superficial gas velocity from 0.1 to 0.7 m/s the polymer produced inside the bubble phase increases from 7.92% to 13.14%. Considering the practical superficial gas velocity range of 0.3–0.6 m/s, the bubble contribution to the reaction rate was estimated to be 11.8–13% which is a quantity that needs to be considered in the model. The presence of carbon monoxide in the feed gases resulted in reduction of polypropylene production rate which highlights the importance of including a carbon monoxide pretreatment facility in the process.

Acknowledgment

The authors thank the Research Council of University of Malaya for its support to this research under research grant (No. RG054/09AET).

References

[1] K.Y. Choi, W.H. Ray, The dynamic behavior of fluidized bed reactors for solid catalyzed gas phase olefin polymerization, Chem. Eng. Sci. 40 (1985) 2261–2278.
[2] N. Mostoufi, H. Cui, J. Chaouki, A comparison of two- and single-phase models for fluidized bed reactors, Ind. Eng. Chem. Res. 40 (2001) 5526–5532.
[3] A. Kiashemshaki, N. Mostoufi, R. Sotudeh-Gharebagh, Two-phase modeling of the gas phase polyethylene fluidized bed reactor, Chem. Eng. Sci. 61 (2006) 3997–4006.
[4] R. Jafari, R. Sotudeh-Gharebagh, N. Mostoufi, Modular simulation of fluidized bed reactors, Chem. Eng. Technol. 27 (2004) 123–129.
[5] J.J. Zacca, J.A. Debling, W.H. Ray, Reactor residence time distribution effects on the multistage polymerization of olefins-I. Basic principles and illustrative examples, polypropylene, Chem. Eng. Sci. 51 (21) (1996) 4859–4886.
[6] Y.M. Harshe, R.P. Utikar, V.V. Ranade, A computational model for predicting particle size distribution and performance of fluidized bed polypropylene reactor, Chem. Eng. Sci. 59 (2004) 5145–5156.
[7] W.H. Ray, On the mathematical modeling of polymerization reactors, J. Macromol. Sci. Rev. Macromol. Chem. Phys. C8 (1972) 1.

[8] R.A. Hutchinson, C.M. Chen, W.H. Ray, Polymerization of olefins through heterogeneous catalysis X: modeling of particle growth and morphology, J. Appl. Polym. Sci. 44 (1992) 1389–1414.
[9] K.B. McAuley, J.F. MacGregor, A.E. Hamilec, A kinetic model for industrial gas-phase ethylene copolymerization, AIChE J. 36 (1990) 837–850.
[10] K.B. McAuley, J.P. Talbot, T.J. Harris, A comparison of two phase and well-mixed models for fluidized bed polyethylene reactors, Chem. Eng. Sci. 49 (1994) 2035–2045.
[11] R.A. Hutchinson, W.H. Ray, Polymerization of olefins through heterogeneous catalysis: VII. Particle ignition and extinction phenomena, J. Appl. Polym. Sci. 34 (2) (1987) 657–676.
[12] H. Hatzantonis, H. Yiannoulakis, A. Yiagopoulos, C. Kiparissides, Recent developments in modeling gas-phase catalyzed olefin polymerization fluidized-bed reactors: the effect of bubble size variation on the reactor's performance, Chem. Eng. Sci. 55 (16) (2000) 3237–3259.
[13] A.S. Ibrehem, M.A. Hussain, N.M. Ghasem, Mathematical model and advanced control for gas-phase olefin polymerization in fluidized-bed catalytic reactors, Chin. J. Chem. Eng. 16 (1) (2008) 84–89.
[14] N.P. Khare, B. Luca, K.C. Seavey, Y.A. Liu, Steady-state and dynamic modeling of gas-phase polypropylene processes using stirred-bed reactors, Ind. Eng. Chem. Res. 43 (2004) 884–900.
[15] J.B.P. Soares, A.E. Hamielec, Deconvolution of chain-length distribution of linear polymers made by multiple-site-type catalyst, Polymer 36 (1995) 2257–2264.
[16] Y.V. Kissin, Isospecific Polymerization of Olefins with Heterogeneous Ziegler–Natta Catalysts, Spinger-Verlag, New York, 1985.
[17] A.B. Carvalho de, P.E. Gloor, A.E. Hamielec, A kinetic mathematical model for heterogeneous Ziegler–Natta copolymerization, Polymer 30 (1989) 280–296.
[18] A. Alshaiban, Active site identification and mathematical modeling of polypropylene made with Ziegler–Natta catalysts, M.S. Thesis, University of Waterloo, 2008.
[19] S. Floyd, K.Y. Choi, T.W. Taylor, W.H. Ray, Polymerization of olefins through heterogeneous catalysts. III. Polymer particle modelling with an analysis of intraparticle heat and mass transfer effects, J. Appl. Polym. Sci. 32 (1986) 2935–2960.
[20] Z.H. Luo, P.L. Su, D.P. Shi, Z.W. Zheng, Steady-state and dynamic modeling of commercial bulk polypropylene process of Hypol technology, Chem. Eng. J. 149 (2009) 370–382.
[21] F.A.N. Fernandes, L.M.F. Lona, Heterogeneous modeling for fluidized-bed polymerization reactor, Chem. Eng. Sci. 56 (2001) 963–969.
[22] H.P. Cui, N. Mostoufi, J. Chaouki, Characterization of dynamic gas–solid distribution in the fluidized beds, Chem. Eng. J. 79 (2000) 135–143.
[23] M. Alizadeh, N. Mostoufi, S. Pourmahdian, R. Sotudeh-Gharebagh, Modeling of fluidized bed reactor of ethylene polymerization, Chem. Eng. J. 97 (2004) 27–35.
[24] A. Kiashemshaki, N. Mostoufi, R. Sotudeh-Gharebagh, S. Pourmahdian, Reactor modeling of gas-phase polymerization of ethylene, Chem. Eng. Technol. 27 (2004) 1227–1232.
[25] A. Sarvaramini, N. Mostoufi, R. Sotudeh-Gharebagh, Influence of hydrodynamic models on dynamic response of the fluidized bed polyethylene reactor, Int. J. Chem. Reactor Eng. 6 (2008) A55.
[26] R. Habibi, S. Hajizadeh, R. Sotudeh-Gharebagh, N. Mostoufi, Two-phase sequential simulation of a fluidized bed reformer, Chem. Eng. Technol. 31 (2008) 984–989.
[27] H.S. Fogler, Elements of Chemical Reaction Engineering, fourth ed., Prentice Hall, 2005.
[28] D. Kunni, O. Levenspiel, Fluidization Engineering, second ed., Butterworth-Heinmann, Boston, MA, 1991.
[29] A. Lucas, J. Arnaldos, J. Casal, L. Puigjaner, Improved equation for the calculation of minimum fluidization velocity, Ind. Eng. Chem. Process. Des. Dev. 25 (1986) 426–429.